Turkish Journal of Electrical Engineering & Computer Sciences

http://journals.tubitak.gov.tr/elektrik/

Research Article

Turk J Elec Eng & Comp Sci
(2015) 23: 1913 – 1929

doi:10.3906/elk-1403-177

Capacity allocation of hybrid solar-wind energy system based on discrete probabilistic method

Cheng-jin YE[1,*], Wei-dong LIU[1], Xu-hua FU[1], Lei WANG[1], Min-xiang HUANG[2]
[1]Economy Research Institute of State Grid Zhejiang Electric Power Company, Hangzhou, P.R. China
[2]College of Electrical Engineering, Zhejiang University, Hangzhou, P.R. China

Received: 18.03.2014 • **Accepted/Published Online:** 08.07.2015 • **Printed:** 30.11.2015

Abstract: Complementary renewable energies like wind and solar power may be more sufficient to satisfy reliability requirements. This paper proposes a quantitative capacity allocation method of a hybrid wind and solar energy system. First, discrete probability distributions are established to model the random factors including the volatility of power outputs and the failure of components. Then a multiobjective optimization model is formulated with objectives of minimization of the total investment, the nodal voltages violating limits probability, and power supply inadequacy probability. For the purpose of fast probability computing with a satisfactory precision degree, an innovative probabilistic load flow algorithm is introduced, which deals with means and increments of random variables separately and uses cumulants as well as Gram–Charlier series to obtain probabilistic distributions of state variables. A modified parallel elitist nondominated sorting genetic algorithm II is used to search the Pareto optimal configuration solutions.

Key words: Wind turbine, photovoltaic, capacity allocation, discrete probability distribution, multiobjective optimization, probabilistic load flow, NSGA-II

1. Introduction

With the increasing exhaustion of fossil fuel and the rapidly growing energy consumption, renewable energy (RE) generation technologies show great advantages and significant potential for development, especially in relatively isolated areas such as remote deserts or offshore islands that are usually abundant in wind and solar resources but suffer from problems in long-distance electric transmission.

Compared with conventional power such as hydropower and thermal generation, the most significant characteristic of RE is the randomness and intermittency of the power output, which will greatly affect the power quality and even cause power inadequacy problems [1]. Many studies have showed that a relatively stable output performance can be achieved when different REs are employed synergistically. The most typical example is the hybrid wind and solar energy conversion system. Generally, wind turbine generators (WTGs) have higher power output rates in the night, because of the better wind regime. Photovoltaic (PV) arrays, on the other hand, can only generate during daylight hours. Complementary REs like WTGs and PV arrays can be more efficacious to meet the reliability requirements of power consumers. Thus, the optimal proportion allocation of different REs is of significant theoretical and practical value in autonomous energy conversion system planning [2,3].

As reported in most of the current studies [4,5], system simulation is executed and system state parameters

*Correspondence: yechenjing@zju.edu.cn

are compared under different RE connection modes and capacities. Obviously, this deterministic enumeration method suffers from a cumbersome workload and does not reveal the overall situation and internal rules of the system. Application of probabilistic analysis to calculate the probabilistic distributions (PDs) of some system state variables is an approach to solve this problem.

Monte Carlo simulation is a widely used probabilistic method [6]. Generally, to get meaningful results, thousands of simulations are repeatedly run during a Monte Carlo procedure. Though the Monte Carlo method may be capable of providing relatively higher accuracy, the time-consuming disadvantage makes it not suitable to use in realistic systems. It is mainly used by researchers for the purpose of comparison.

Probabilistic load flow (PLF), proposed in 1974 [7], is a promising probabilistic analytical method. In classic PLF study [8,9], the input variables are modeled as random variables respecting some PDs, and after linearization, the power flow state vector can be expressed as a linear combination of input variables. Therefore, a convolution technique can be used to calculate the PDs of objective variables such as voltage profile and branch flow. Extended PLF proposed in [10,11] replaced convolution calculations with simple arithmetic calculations based on some significant properties of cumulants. In addition, Laguerre polynomials and Gram–Charlier expansion [11,12] were introduced to approximate the probabilistic density function (PDF) of objective variables in one run, which greatly improved the calculation speed while maintaining enough accuracy.

Many uncertain factors in power systems are discontinuous, such as the condition of a WTG, which has two states, normal and failure, and can only be modeled as a discrete random variable respecting a PD in the form of a set of ordered pairs, rather than a continuous PDF. On the other hand, computer-aided calculation of the joint PD or convolution of mixed discrete and continuous variables is rather complex. Thus, taking discrete factors into consideration, classic PLF is still faced with certain difficulties in practice.

Until recently, extensive existing studies on this hybrid wind and solar system configuration issue were all limited to single-objective optimization. The most frequently mentioned method is to search the tangent point of the trade-off curve and the cost line, which specifically models the total cost as an objective function and reliability indexes such as the loss of power supply probability as constraints [13–15]. It must be noted that, in many cases, modeling the configuration of hybrid renewable energies system as a multiobjective optimization problem is more appropriate.

In this paper, a multiobjective configuration method based on discrete probabilistic distribution and an innovative PLF algorithm is proposed, which offers an objective and quantitative method for capacity allocation of different REs.

2. A multiobjective optimization model

2.1. Decision variables

First, the core issue of the previous problem is the capacity allocation of various REs. On the other hand, in order to improve voltage quality, reactive power compensation equipment is also necessary for a hybrid system.

Therefore, the decision variables of the optimization problem are the number and unit capacity of WTGs or reactive power compensation devices and the number and unit area of PV modules, denoted by N_i and p_i respectively.

2.2. Objective functions

The purpose of hybrid RE conversion system configuration is to achieve balance between the overall system performance and the total investment without violating the relevant constraints of safe and stable operation. Thus, the following three objective functions are adopted:

1) The total investment of power supply system:

$$OB_1 = \sum_i N_i \left(k_{1i} + p_i k_{2i}\right), \tag{1}$$

where k_{1i} and k_{2i} are the fixed and variable cost coefficients of the ith RE generation or reactive power compensation devices.

2) The nodal voltages violating limits probability:

$$OB_2 = 1 - \prod_i^{\Phi} P_r \left[V_i^{\min} < V_i < V_i^{\max}\right], \tag{2}$$

where V_i is the voltage of node i, and $V_i^{\min}$ and $V_i^{\max}$ are the lower and upper limits of V_i. Φ is the set of the nodes. P_r [A] in Eq. (2) and the following sections of the paper represents the probability of event A. Eq. (2) quantitates the system volatility.

3) The power inadequacy probability:

$$OB_3 = P_r \left[\sum_i X_i \le Y\right], \tag{3}$$

where X_i is the active power output of the ith RE generation device and Y represents the load power. Eq. (3) quantitates the energy adequacy degree of the system, which respectively represents the electric supply outage probability for isolated systems and the probability of absorbing electricity from the main power grid for interconnected systems.

The essential issue of the multiobjective optimization model is the minimization of OB_1, OB_2, and OB_3 as simultaneously as possible. In this paper, discrete PDs are used to represent random factors of the system, and an improved PLF algorithm is proposed to conveniently calculate OB_2 and OB_3, on this basis of which the Pareto optimal combination of N_i and p_i are searched through the multiobjective stochastic algorithm PNSGA-II.

3. Probability distribution of power injections

3.1. Probabilistic analysis of WTG

The wind velocity in each time-frame is treated as a random variable, which is usually considered to respect the following PDF of Weibull distribution [16]:

$$F_{r1}(v) = \frac{\pi}{c}\left(\frac{v}{c}\right)^{\pi-1} \exp\left[-\left(\frac{v}{c}\right)^{\pi}\right], \tag{4}$$

where v is the wind speed in m/s, π is the shape parameter, and c is the scale parameter.

Power output of a WTG farm is a random variable subject to the parameters of the WTG and wind speed. Piecewise curves have been commonly used to represent the WTG output characteristics [13–16]. Assumptions are made that all the WTGs of the farm are of identical parameters and wind speed. The power capacity available from the WTG farm at wind speed v, denoted by x_1, can be expressed using the following function:

$$x_1 = \psi(v) = \begin{cases} 0, & v \le v_c or v \ge v_F \\ N_1 p_1 \frac{v - v_c}{v_R - v_c}, & v_c \le v \le v_R \\ N_1 p_1, & v_R \le v \le v_F \end{cases}, \tag{5}$$

where N_1 is the number of WTGs, p_1 is the rated power capacity of a WTG, and v_c, v_R, and v_F are the cut-in, rated, and cut-out wind speeds, respectively.

Discretization is executed on the continuous power curve to obtain n separate output power values: $x_1^*(i)$, (i = 1,2,...,n). The discretization strategy is shown in Figure 1 [16], where $x_1^*(1) = 0$ and the corresponding wind speed range is less than v_c or greater than v_F, and $x^*(n) = N_1 p_1$ and the corresponding wind speed range is from v_R to v_F. The curve between v_c and v_R is evenly divided into $n-2$ intervals, and the interval length is $a = (v_R - v_c)/(n-2)$. For each interval, for example for the ith interval (i = 2,3,...,$n-1$), the corresponding wind speed range is from $v_c - (i-2)a$ to $v_c - (i-1)a$, and $x_1^*(i)$ is assigned to be the middle value of $\psi(v_c - (i-2)a)$ and $\psi(v_c - (i-1)a)$.

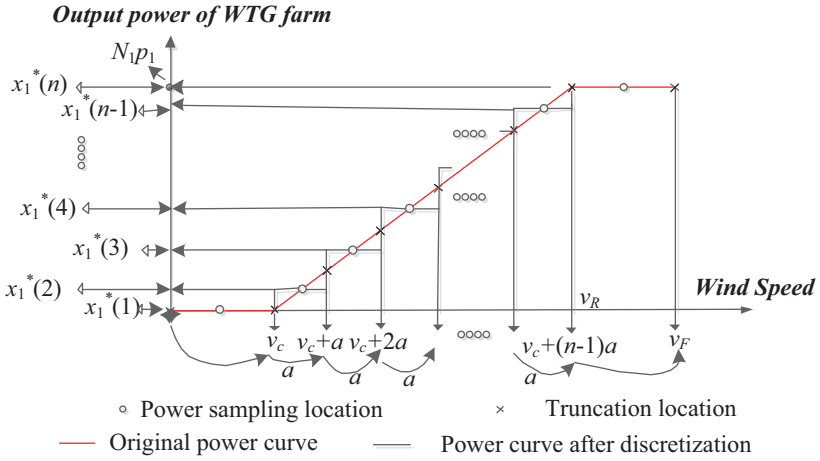

Figure 1. Sampling on the WTG power output curve.

The PD of x_1^* is a set of ordered pairs, denoted as $D(x_1^*)$, which is given by the following equation.

$$D(x_1^*) = \{x_1^*(i), \Pr[x_1^*(i)]\}, i = 1,2,3,\cdots,n$$
$$x_1^*(i) = \begin{cases} 0, i = 1 \\ \psi(v_c + (i-1.5)a), i = 2,3,\cdots,n-1 \\ N_1 p_1, i = n \end{cases} ; \Pr[x_1^*(i)] = \begin{cases} \int_0^{v_c} F_{r1}(v)dv + \int_{v_F}^{\infty} F_{r1}(v)dv, i = 1 \\ \int_{v_c+(i-2)a}^{v_c+(i-1)a} F_{r1}(v)dv, i = 2,3,\cdots,n-1 \\ \int_{v_R}^{v_F} F_{r1}(v)dv, i = n \end{cases} \quad (6)$$

Due to possible component failure, actual power output of the WTG farm is generally smaller than the theoretical capacity at current wind speed. To simplify the analysis, the outage rate of each WTG is denoted as λ. We introduce a random variable S_1, the availability rate of WTGs, which can be expressed as:

$$S_1(i) = \frac{P_v(i)}{P_v}, i = 0,1,\cdots,N_1. \quad (7)$$

At the given wind speed v, $P_v(i)$ and P_v indicate the active power output when i WTGs are available and the power output when all the WTGs are available, respectively. Obviously, S_1 respects the binomial distribution and the PD of S_1 is given as follows.

$$D(S_1) = \{S_1(i), \Pr[S_1(i)]\}, i = 0,1,2,\cdots,N_1$$
$$S_1(i) = \frac{i}{N_1}, \Pr[S_1(i)] = C_{N_1}^i \lambda^{N_1 - i}(1-\lambda)^i \quad (8)$$

Actual power output of the WTG farm, denoted by X_1, is modeled as a two-state Markov process of the maximum output capacity at the current wind speed and the possible forced outage. The PD of X_1 can be expressed as the convolution by the PDs of random variables x_1^* and S_1:

$$D\left(X_1\right)=\left\{X_1\left(k\right),\Pr\left[X_1\left(k\right)\right]\right\}=D\left(x_1^*\right)\otimes D\left(S_1\right),k=0,1,2,\cdots,N_1n. \tag{9}$$

3.2. Probabilistic analysis of PV modules

In each time-frame, the solar irradiance is supposed to follow a β-distribution. Since the power output of PV modules is proportional to the solar irradiance, it can be modeled as a random variable x_2, which respects a β-distribution in the same form given by the following PDF [13–16]:

$$F_{r2}\left(x_2\right)=\frac{\Gamma\left(\alpha+\beta\right)}{\Gamma\left(\alpha\right)\Gamma\left(\beta\right)}\left(\frac{x_2}{P_M}\right)^{\alpha-1}\left(1-\frac{x_2}{P_M}\right)^{\beta-1}, \tag{10}$$

where α and β are shape parameters, and $\Gamma(\ )$ is the gamma function. Given N_2 solar modules, each with an area p_2 and efficiency η, and the maximum solar irradiance is r_m in $\mathrm{W/m^2}$, the maximum active power available from the modules, denoted by P_M, is evaluated using the function $P_M=r_mN_2p_2\eta$.

Let x_2^* be the discrete form of x_2; then the PD of x_2^* is a set of ordered pairs, denoted as $D(x_2^*)$, which is given by:

$$D\left(x_2^*\right)=\left\{x_2^*\left(i\right),\Pr\left[x_2^*\left(i\right)\right]\right\},i=1,2,3,\cdots,n. \tag{11}$$

As shown in Figure 2, the power range from 0 to P_M is uniformly divided into n separate intervals, and the power values can be expressed as:

$$x_2^*\left(i\right)=\frac{\left(i-0.5\right)P_M}{n},i=1,2,3,\cdots,n. \tag{12}$$

The probabilities of the discrete power values are obtained by integrating:

$$\Pr\left[x_2^*\left(i\right)\right]=\int_{\frac{(i-1)P_M}{n}}^{\frac{iP_M}{n}}F_{r2}\left(x_2\right)dx_2. \tag{13}$$

The forced outage rate of each module is denoted by ρ, and then the availability rate of PV modules S_2 respects the binomial distribution and the PD can be expressed as:

$$D\left(S_2\right)=\left\{S_2\left(i\right)=\frac{i}{N_2},\Pr\left[S_2\left(i\right)\right]=C_{N_2}^{i}\rho^{N_2-i}\left(1-\rho\right)^{i}\right\},i=0,1,\cdots,N_2. \tag{14}$$

The actual power output of PV modules is denoted as X_2, and the PD of X_2 is the convolution by $D(x_2^*)$ and $D(S_2)$.

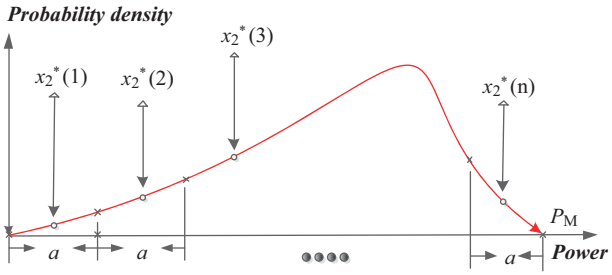

Figure 2. Sampling on the PDF curve of PV power.

3.3. Probabilistic analysis of compensators

In this paper, reactive power compensators are deployed on the generation bus. The controlling strategy of the compensators is cutting in or out capacitors according to the value of RE active power output automatically to ensure the ratio of reactive and active power of the system stays as constant as possible. This strategy can be expressed as:

$$\frac{z}{X} = \alpha, \tag{15}$$

where X is the active power output of WTGs and PV modules, z is the reactive power injection of compensators, and α is a constant parameter controlling the power factor of the generation side. The commonly used compensator consists of several capacitors connected in parallel, which cannot realize step-less adjustment, so z can be written as z^*. Shown in Eq. (15), z^* is a discrete random variable subject to X.

The PD of RE active power output is expressed as the following set of ordered pairs:

$$D\left(X^*\right) = \left\{X^*\left(i\right), \Pr\left[X^*\left(i\right)\right]\right\}, i = 1, 2, 3, \cdots, M. \tag{16}$$

Given N_3 capacitors connected in parallel, each capacitor has the same capacity of p_3. Obviously, $X^*(\mathrm{M})$ is the maximum active power output of REs, which is divided into N_3 intervals evenly, and the interval length is $X^*(\mathrm{M})/N_3$. The PD of z^* can be expressed as follows.

$$\begin{aligned} &D\left(z^*\right) = \left\{z^*\left(k\right), \Pr\left[z^*\left(k\right)\right]\right\}, k = 1, 2, 3, \cdots, N_3 \\ &z^*\left(k\right) = kp_3; \Pr\left[z^*\left(i\right)\right] = \sum \Pr\left[X^*\left(i\right)\right] \\ &\tfrac{(k-1)X^*(M)}{N_3} \le X^*\left(i\right) \le \tfrac{kX^*(M)}{N_3}, i = 1, 2, 3, \cdots, M \end{aligned} \tag{17}$$

Considering the forced outage rate of the capacitor, the PD of the actual reactive power output can be calculated by convolution calculation.

3.4. Probabilistic analysis of load

The load referred to in planning is a predictive value; the actual load is a random variable, denoted as y. An assumption is made that the load has a normal PDF [17]:

$$F_y\left(y\right) = \frac{1}{\sqrt{2\pi}\sigma_y} \exp\left(-\frac{\left(y-\mu_y\right)^2}{2\sigma_y^2}\right). \tag{18}$$

As shown in Figure 3, the load range from $\mu - 3\sigma$ to $\mu + 3\sigma$ is evenly divided into n intervals, and the interval length is $a = 6\sigma \,/\, (n-1)$. Starting from $\mu - 3\sigma$, a discrete load value $y^*(i)$ $(i = 1,2,\ldots,n)$ is sampled every length a. The integration of $F_y(y)$ in the range of $y^* - 0.5a$ to $y^* + 0.5$ is considered as the probability of $y^*(i)$.

$$\begin{aligned} &D\left(y^*\right) = \left\{y^*\left(i\right), \Pr\left[y^*\left(i\right)\right]\right\} \\ &y^*\left(i\right) = (\mu - 3\delta) + \frac{6\delta(i-1)}{n-1}; \Pr\left[y^*\left(i\right)\right] = \int_{(\mu-3\delta)+\frac{6\delta(i-1.5)}{n-1}}^{(\mu-3\delta)+\frac{6\delta(i-0.5)}{n-1}} F_y\left(y\right)dy, i = 1, 2, 3, \cdots, n \end{aligned} \tag{19}$$

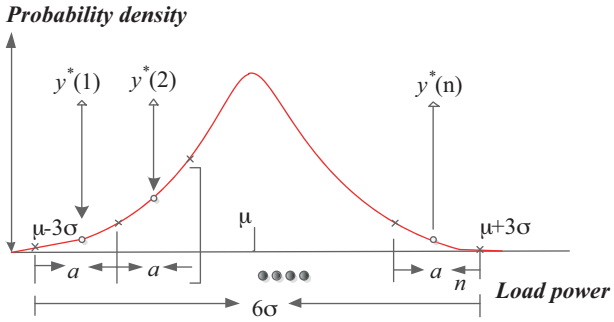

Figure 3. Sampling on the load PDF curve.

4. Theoretical background

4.1. Probabilistic load flow algorithm

For a given system configuration, the nodal power flow equations can be expressed as:

$$W = f(X), \tag{20}$$

where $f()$ is the power injection function, X is the system state vector including nodal voltages and angles, and W is the real and reactive power injections vector. The input vector and state vector can be expressed as the sum of means and the increments: $W = W_0 + \Delta W$, $X = X_0 + \Delta X$. Here, ΔW and ΔX are random variables respecting some specific PDs.

Expanding nodal power flow equations around X_0 using Taylor series and omitting the high-order items, Eq. (20) can be expressed as follows:

$$W_0 + \Delta W = f(X_0 + \Delta X) = f(X_0) + J_0 \Delta X + \frac{J_0' \Delta X^2}{2!} + \frac{J_0'' \Delta X^3}{3!} \cdots \approx f(X_0) + J_0 \Delta X, \tag{21}$$

where J_0 is the Jacobian matrix of the last iteration in the Newton–Raphson procedure. As $W_0 = f(X_0)$, the state increment vector can be expressed as:

$$\Delta X \approx J_0^{-1} \Delta W = S_0 \Delta W, \tag{22}$$

where S_0 is the sensitivity matrix or the inverse matrix of J_0; J_0 has been triangular factorized in the Newton–Raphson procedure, so S_0 is easy to obtain. As ΔX is a polynomial in a set of random variables ΔW, the PD of ΔX can be expressed as the convolution of ΔW.

4.2. Gram–Charlier series and properties of moments and cumulants

Given a discrete random variable ζ, whose mean value is m and standard deviation is σ, according to the Gram–Charlier series the cumulative probability function (CDF) of the standardized variable $(\zeta - m)/\sigma$ can be expressed as [11]:

$$F(x) = \Phi(x) + \frac{c_1}{1!}\Phi'(x) + \frac{c_2}{2!}\Phi''(x) + \frac{c_3}{3!}\Phi'''(x) + \cdots, \tag{23}$$

where (x) is the CDF of the standard normal distribution. Here, we use a Gram–Charlier series from 3 to 9 in order. We denote the vth order central moment of ζ as $\beta_v(\zeta)$. Coefficient c_v is a polynomial in $\beta_v(\zeta)$ [18].

$$\begin{aligned}
&c_0 = 1; c_1 = c_2 = 0;\\
&c_3 = -\tfrac{\beta_3(\zeta)}{\sigma^3}; c_3 = \tfrac{\beta_4(\zeta)}{\sigma^4} - 3;\\
&c_5 = -\tfrac{\beta_5(\zeta)}{\sigma^5} + 10\tfrac{\beta_3(\zeta)}{\sigma^3}; c_5 = \tfrac{\beta_6(\zeta)}{\sigma^6} - 15\tfrac{\beta_4(\zeta)}{\sigma^4} + 30;\\
&\cdots\cdots
\end{aligned} \tag{24}$$

Here, we denote the vth order origin moment and cumulant of ζ as $\alpha_v(\zeta)$, $\zeta^{(v)}$. The relationship between origin and central moments can be expressed as follows [18].

$$\begin{aligned}
&\beta_0(\zeta) = 1; \beta_1(\zeta) = 0;\\
&\beta_2(\zeta) = \alpha_2(\zeta) - \alpha_1(\zeta)^2;\\
&\beta_3(\zeta) = \alpha_3(\zeta) - 3\alpha_1(\zeta)\alpha_2(\zeta) + 2\alpha_1(\zeta)^3;\\
&\cdots\cdots\\
&\beta_v(\zeta) = \sum_{j=0}^{v} C_v^j \alpha_{v-j}(\zeta)(-\alpha_1(\zeta))^j
\end{aligned} \tag{25}$$

It is seen that $\zeta^{(v)}$ is a polynomial in $\alpha_v(\zeta)$ [18].

$$\begin{aligned}
&\zeta^{(1)} = \alpha_1(\zeta);\\
&\zeta^{(2)} = \alpha_2(\zeta) - \alpha_1(\zeta)\zeta^{(1)};\\
&\zeta^{(3)} = \alpha_3(\zeta) - 2\alpha_1(\zeta)\zeta^{(2)} - \alpha_2(\zeta)\zeta^{(1)};\\
&\cdots\cdots\\
&\zeta^{(r+1)} = \alpha_{r+1}(\zeta) - \sum_{j=1}^{r} C_r^j \alpha_j(\zeta)\zeta^{(r-j+1)}
\end{aligned} \tag{26}$$

Property: If y_1, y_2, y_3,..., y_n are independent random variables with the vth order cumulants $y_1^{(v)}$, $y_2^{(v)}$, $y_3^{(v)}$,..., $y_n^{(v)}$, respectively, the vth order cumulant of the sum variable $x = \lambda_1 y_1 + \lambda_2 y_2 + \lambda_3 y_3 + \ldots + \lambda_n y_n$ is thus given by [11]:

$$x^{(v)} = \lambda_1^v y_1^{(v)} + \lambda_2^v y_2^{(v)} + \cdots + \lambda_n^v y_n^{(v)}, \tag{27}$$

where λ_i $(i = 1,2,3,\ldots,n)$ are constant coefficients and λ_i^v is the vth power of λ_i.

5. A modified probabilistic load flow algorithm

5.1. The procedure of a modified PLF

The basic idea of the improved PLF algorithm is to deal with the means and increments of random variables separately and transform and calculate the cumulants of increments through their moments. The procedure of approximating the PDF of V_i and calculating the probability of V_i violating its limits is summarized as follows:

Step 1: Discretize continuous power curves or PDF curves to establish the PDs of the output power of REs in the form of a set of ordered pairs. Taking availability rate into consideration, calculate the PDs of actual output power of WTGs, PV modules, compensators, and load by convolution.

Step 2: Calculate the means and PD of the increments of the output power of WTGs, PV modules, compensators, and load. For example, if the PD of the output power of some RE generation device is:

$$D\left(X^*\right)=\left\{X^*\left(i\right),\Pr\left[X^*\left(i\right)\right]\right\},i=1,2,3\cdots,n, \tag{28}$$

then its power mean, denoted by m, is calculated by:

$$m=\sum_{i=1}^{n}X^*\left(i\right)\Pr\left[X^*\left(i\right)\right]. \tag{29}$$

The PD of power increment is expressed as follows.

$$D\left(\Delta X^*\right)=\left\{\Delta X^*\left(i\right)=X^*\left(i\right)-m,\Pr\left[\Delta X^*\left(i\right)\right]=\Pr\left[X^*\left(i\right)\right]\right\},i=1,2,3,\cdots,n$$

Step 3: Calculate the origin moments of the power increments of WTGs, PV modules, compensators, and load, denoted as $\alpha_v(\Delta X*)$:

$$\alpha_v\left(\Delta X^*\right)=\sum_{i=1}^{n}\Pr\left[X^*\left(i\right)\right]\left(X^*\left(i\right)-m\right)^v. \tag{30}$$

Calculate the central moments and cumulants of power increments of WTGs, PV modules, compensators, and load according to Eqs. (25) and (26), denoted by $\beta_v(\Delta X*)$ and $\Delta X*^{(v)}$, respectively.

Step 4: Regulate the output power of WTGs, PV modules, compensators, and load to their corresponding means calculated in Step 2. Execute power flow calculation to obtain the node voltage means and the sensitivity matrix of the last iteration, denoted by $V_i^{mean}\left(i=1,2,3,\ldots\right)$ and S, respectively.

Step 5: Nodal active and reactive power injections are linear combinations of the output power of WTGs, PV modules, compensators, and load, as are the nodal power injection increments. Based on Eq. (27), calculate the cumulants of power injection increments with cumulants of the corresponding RE or load power increments obtained in Step 3.

Step 6: The power flow equation of the last iteration in Step 4 is as follows.

$$\begin{bmatrix}\Delta\theta\\ \Delta\mathbf{V}/\mathbf{V}\end{bmatrix}=\begin{bmatrix}\mathbf{J}_{\theta P} & \mathbf{J}_{\theta Q}\\ \mathbf{J}_{VP} & \mathbf{J}_{VQ}\end{bmatrix}\begin{bmatrix}\Delta\mathbf{V}\\ \Delta\mathbf{Q}\end{bmatrix} \tag{31}$$

Node voltage increment vector $\Delta\mathbf{V}$ is a linear combination of nodal power injection increment vector $\Delta\mathbf{P}$ and $\Delta\mathbf{Q}$. According to Eq. (33), the v-order cumulant of the voltage increment of node i, denoted by $\Delta V_i^{(v)}$, can be calculated by:

$$\Delta V_i^{(v)}=\sum_j\left(\mathbf{J}_{VP}(i,j)V_i^{mean}\right)^v\Delta P_j^{(v)}+\sum_j\left(\mathbf{J}_{VQ}(i,j)V_i^{mean}\right)^v\Delta Q_j^{(v)}, \tag{32}$$

where $\mathrm{J}_{VP}(i,j)$ and $\mathrm{J}_{VQ}(i,j)$ are elements of $\boldsymbol{S}$, V_i^{mean} is obtained in Step 4, and $\Delta P_j^{(v)}$ and $\Delta Q_j^{(v)}$ are the v-order cumulants of active and reactive nodal power injection increments of node j obtained in Step 5.

Step 7: Compute the central moments of ΔV_i using Eqs. (25) and 26, denoted by $\beta_v(\Delta V_i)$. Calculate the Gram–Charlier expansion coefficients based on Eq. (24). The standardized variable of ΔV_i is denoted as

w. Here, $w = (\Delta V_i - \mu)/\sigma$, and μ and σ are the mean and standard deviation of ΔV_i. CDF of w is acquired using Eq. (23). According to Eq. (26), $\Delta V_i^{(1)} = \alpha_1(\Delta V_i) = \mu$; $\Delta V_i^{(2)} = \alpha_2(\Delta V_i) - \alpha_1^2(\Delta V_i) = \sigma^2$. Thus, μ and σ can be calculated easily based on $V_i^{(1)}$ and $V_i^{(2)}$.

Step 8: The probability of V_i violating its limits is equal to the probability of the voltage increment violating the corresponding limits:

$$1 - \Pr\left\{V_i^{\min} < V_i < V_i^{\max}\right\} = 1 - \Pr\left\{\Delta V_i^{\min} < \Delta V_i < \Delta V_i^{\max}\right\}, \tag{33}$$

where $\Delta V_i^{\min}$ and $\Delta V_i^{\max}$ are the upper and lower limits of ΔV_i, and $\Delta V_i^{\min} = V_i^{\min} - \mu$, $\Delta V_i^{\max} = V_i^{\max} - \mu$; μ is the mean of ΔV_i obtained in Step 7. Given the CDF of w in Step 7, denoted as $F_1(w)$, the probability of V_i violating its limits can be calculated as follows.

$$1 - \Pr\left\{\Delta V_i^{\min} < \Delta V_i < \Delta V_i^{\max}\right\} = 1 - \left[F_1\left(\frac{\Delta V_i^{\max} - \Delta V_i^{(1)}}{\sqrt{\Delta V_i^{(2)}}}\right) - F_1\left(\frac{\Delta V_i^{\min} - \Delta V_i^{(1)}}{\sqrt{\Delta V_i^{(2)}}}\right)\right] \tag{34}$$

Similarly, the power supply inadequacy probability OB_3 can be calculated as follows:

Step 1: The difference between generation power and load is a random variable, denoted by δ, which is a polynomial in the active power outputs of WTGs, PV modules, and load:

$$\delta = \sum X_i - Y \tag{35}$$

Step 2: Compute the cumulants of δ using the cumulants of X_i and Y, and then obtain the CDF of the standardized variable of δ using Gram–Charlier expansion, denoted as $F_2(w)$. OB_3 can be calculated as follows:

$$OB_3 = \Pr(\delta \le 0) = F_2\left(-\frac{\delta^{(1)}}{\sqrt{\delta^{(2)}}}\right). \tag{36}$$

5.2. A master-slave parallel NSGA-II on MPI

The NSGA-II and its detailed procedure can be found in [19]. Due to the heavy task of power flow calculation as well as convolution and derivation of high order, the hybrid wind and solar energy conversion system configuration is inevitably data-intensive. To solve this problem, parallel modification of the NSGA-II program structure on the Message Passing Interface (MPI) platform is a method worth trying. Figure 4 shows the parallel strategy used [20].

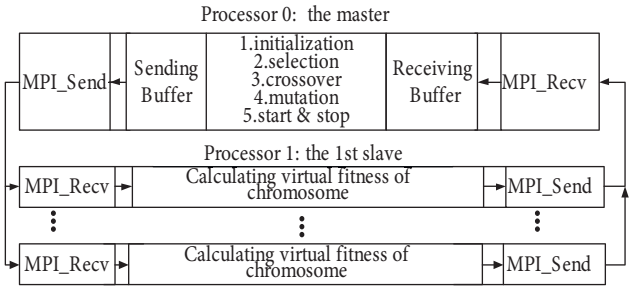

Figure 4. Master-slave topology of PNSGA-II.

5.3. Optimal solution selection

Due to the vagueness of human thoughts, the optimal solution selection method based on subjective preference is of significant limitation. This paper proposes a selection method based on fuzzy membership and variance weight.

Membership indicates the optimization degree of objective functions. Here, fuzzy theory is applied to each function value of optimal solutions for the fuzzy membership. The fuzzy membership of the jth objective function of the ith optimal solution Φ_{ij} is calculated as:

$$\Phi_{ij}=\frac{OB_j^{\max}-OB_{ij}}{OB_j^{\max}-OB_j^{\min}}, i=1,2,\cdots,n_1; j=1,2,\cdots,n_2, \tag{37}$$

where n_1 is the number of optimal solutions, n_2 is the number of objective functions, OB_{ij} is the jth objective function value of the ith optimal solution, and $OB_j^{\max}$ and $OB_j^{\min}$ are the minimum and maximum values of the jth objective function in the optimization process. Objective function values are normalized to a real between 0 and 1 by Eq. (37).

In this paper, we quantitate the quality of a Pareto optimal solution through its weighted sum of fuzzy memberships. A weight assignment method based on the variance is introduced to reduce subjectivity:

$$w_j=\frac{\sum_{i=1}^{n_1}\sum_{k=1}^{n_1}\left(\Phi_{ij}-\Phi_{kj}\right)^2}{\sum_{j=1}^{n_2}\left[\sum_{i=1}^{n_1}\sum_{k=1}^{n_1}\left(\Phi_{ij}-\Phi_{kj}\right)^2\right]}, \tag{38}$$

where w_j is the weight of the jth objective function. $\sum_{i=1}^{n_1}\sum_{k=1}^{n_1}\left(\Phi_{ij}-\Phi_{kj}\right)^2$ is the fuzzy membership variance of the jth objective function. The proposed weighting method naturally respects the constraint, $\sum_{j=1}^{n_2}\omega_j=1$, and gives the objective function of a larger fluctuation of optimization results a bigger weight. Specifically, the larger the fuzzy membership variance of OB_j, the larger the weight assigned to OB_j, and vice versa.

The weighted sum of fuzzy memberships of each solution is calculated and used as an unbiased optimal solution indicator:

$$\Theta^i=\sum_{j=1}^{n_2}\Phi_{ij}\omega_j, i=1,2,\cdots,n_1. \tag{39}$$

Θ^i is used as the selection priority value of the ith solution. The solution with the maximum Θ value is regarded as the best unbiased optimal solution.

6. Simulation on an eastern China costal island grid

6.1. Basic parameters

An eastern China costal island grid, which can be simplified to a 7-bus network as shown in Figure 5, is used for simulation.

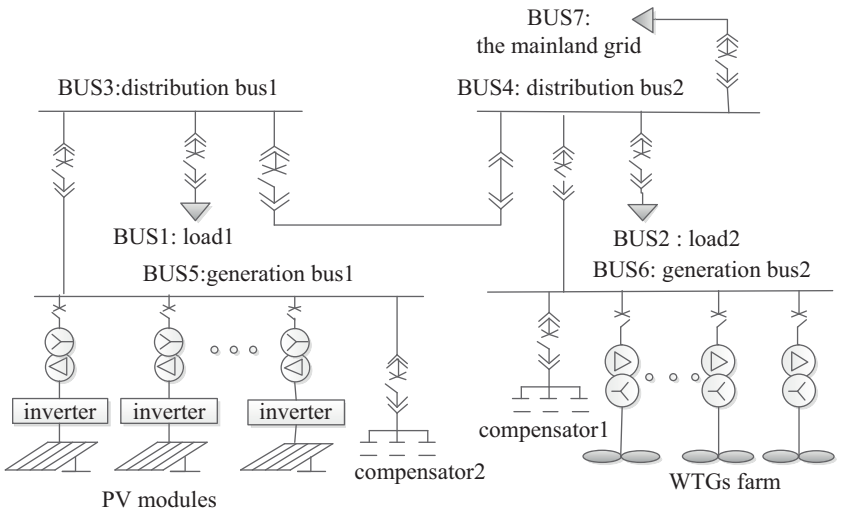

Figure 5. Diagram of the costal island microgrid.

The cut-in, rated, and cut-out wind speed of the WTG is 4, 13, and 23 in m/s, respectively. The photoelectric conversion efficiency is 22.9%. The mean and standard deviation of load 1 and load 2 are $\mu_1 = 2.6$, $\sigma_1 = 0.5$ and $\mu_2 = 2.3$, $\sigma_2 = 0.4$ in MW, respectively. The two loads are considered as a PQ bus with the power factor of 0.8. The upper and lower limits of nodal voltage are 1.3 pu and 0.7 pu, respectively. Based on the data of monthly average wind speed and solar radiation of the island, we get distribution parameters as $k = 10.46$, $c = 6.67$, $\alpha = 2.96$, $\beta = 1.57$, and $r_m = 0.83$ kW/m^2 [17]. The number of sampling points on the continuous power curves or PDF curves is set to 200. Due to the deficiency of actual operation data, the MTTF and MTTR of the WTG and PV module are based on some typical project statistics in Europe [21,22]. The fixed and variable cost coefficients and the upper and lower limits of the decision variables are shown in Table 1.

Table 1. Summary of decision variables and the corresponding limits (¥ = Chinese yuan = US $0.16).

Items	Fixed cost coefficient	Variable cost coefficient	Decision variables		The lower limit	The upper limit
WTG	1×10^5 ¥	0.3×10^4 ¥/kW	Number	N_1	5	50
			Rated power of a WTG/kW	p_1	5	500
PV module	5×10^5 ¥	0.2×10^4 ¥/m^2	Number	N_2	5	100
			Area of a module/m^2	p_2	5	150
Compensator 1	6×10^4 ¥	0.5×10^4 ¥/kvar	Number	N_3	5	30
			Capacity of a capacitor/kvar	p_3	5	150
Compensator 2	6×10^4 ¥	0.5×10^4 ¥/kvar	Number	N_4	3	25
			Capacity of a capacitor/kvar	p_4	5	130

6.2. Pareto optimal solutions

Figure 6 shows the location of population before and after 50 generations of evolution. As can be seen, the population assembling effect is quite obvious with two nondominated fronts appearing.

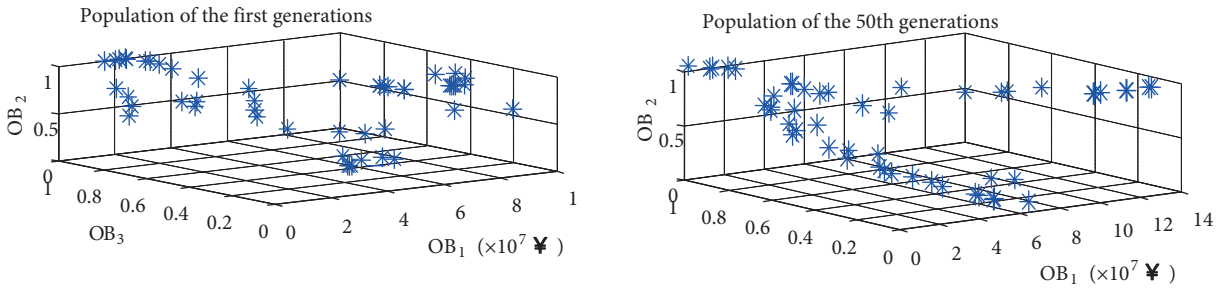

Figure 6. The location of the population.

With the increasing of evolution generation, the proportion of nondominated solutions that are not dominated by others in the population is gradually increasing. After 50 generations of evolution, the inferior solutions that are dominated by others have been eliminated completely.

As can be seen from the location of the population, the three objective functions of the problem are conflicting. This is determined by the characteristics of the multiobjective model. Consider the following two situations:

1) In order to reduce the investment, less capacity of RE generation devices is deployed, which inevitably increases the power supply inadequacy probability.

2) In order to reduce the probability of the node voltage violating its limits, RE generation devices that generate electricity of high volatility should be configured to account for a smaller share of the total generating capacity. Thus, the probability of absorbing electricity from a major power grid increases.

In a word, it is better to meet one objective of the model, inevitably at the expense of the others.

Table 2 shows the Pareto solutions after 50 generations of evolution. Decision-makers can select the final solution from Table 2 according to their preference. For example:

Table 2. A set of Pareto optimal solutions.

Serial number	Decision variables								Objective functions		
	WTGs		PV modules		Compensator 1		Compensator 2		$OB_1(10^4$ ¥)	OB_2	OB_3
	N_1	p_1/kW	N_2	p_2/m^2	N_3	p_3/kvar	N_4	p_4/kvar			
1	62	17	119	500	28	29	20	119	6389.6	17.53%	1.62%
2	31	11	41	38	16	10	3	76	952.6	100.00%	99.31%
3	67	17	134	242	5	44	8	71	4006.8	77.94%	56.96%
4	31	25	128	250	18	21	8	76	3722.6	57.79%	67.66%
5	24	23	125	192	19	10	7	86	2826.8	94.48%	92.85%
6	62	14	102	467	25	10	19	104	5053.2	41.57%	16.03%
7	80	24	27	460	26	110	18	77	6771	14.04%	19.70%
8	43	28	105	499	5	100	12	38	6169.6	5.74%	100.00%
9	29	23	122	218	18	10	6	84	3072.8	84.80%	86.94%
10	65	17	138	285	6	33	9	72	4255.5	61.91%	44.13%

Case 1: If the total investment is required to be less than 1000 $\times$ 10^4 yuan, then solution 2 is selected.

Case 2: If the nodal voltage violating its limits and the power supply inadequacy probability are required to be less than 20% both, and a lower investment is accepted, then solution 1 is selected.

Case 3: With no specific preference, the unbiased solution with the best balance between objectives should be adopted. The weights of objective functions based on membership variance are given in Table 3.

Apparently, solution 1 with the maximum Θ value is selected. This method succeeds in avoiding the blindness of the traditional weighting method.

Table 3. The fuzzy membership of the Pareto solutions and the membership variance and weight of each function.

	Serial number	Membership of OB_1	Membership of OB_2	Membership of OB_3	The selection priority (Θ value)
Pareto Solutions	1	0.0656	0.8749	1.0000	0.71
	2	1.0000	0.0000	0.0070	0.27
	3	0.4751	0.2340	0.4375	0.37
	4	0.5239	0.4478	0.3287	0.42
	5	0.6779	0.0586	0.0727	0.23
	6	0.2952	0.6199	0.8535	0.62
	7	0.0000	0.9119	0.8162	0.64
	8	0.1034	1.0000	0.0000	0.39
	9	0.6356	0.1613	0.1328	0.28
	10	0.4323	0.4041	0.5679	0.47
Variance		0.0979	0.1343	0.1402	null
Weight		0.2629	0.3606	0.3765	null

6.3. Result comparison

The classic PLF algorithm uses a continuous PD to describe the probabilistic characteristic of RE output power; the formula of the k-order origin moment of PV power output respecting the β-distribution is given in [17] as:

$$\alpha_k = \frac{\alpha(\alpha+1)(\alpha+2)\cdots(\alpha+k-1)}{(\alpha+\beta)(\alpha+\beta+1)(\alpha+\beta+2)\cdots(\alpha+\beta+k-1)}. \tag{40}$$

Without considering the failure of PV modules, an error, denoted as $\Delta(i,j)$, is introduced as follows:

$$\Delta(i,j) = \frac{R(i,j) - r(j)}{r(j)} \times 100\%, \tag{41}$$

where $R(i,j)$ is the j-order cumulant of the active power output of the PV modules in the previous case calculated using the discrete method, and i is the number of sampling points. $r(j)$ is the j-order cumulant of the active power output of PV modules in the previous case calculated with Eq. (40).

The error values according to different numbers of sampling points and orders are given in Table 4. Visibly, there is inevitably an error in the cumulant calculated using the discrete methods. The calculation results of the discrete method may be larger or sometimes smaller than the real value. The error increases with the increasing of cumulant order and decreases with the increasing number of sampling points. If 200 points are sampled on the PV PDF curve, the error of the fifth-order cumulant is controlled within 0.5%.

Table 4. Error value of the discrete method proposed in this paper.

i = points number	j = order				
	$j=1$	$j=2$	$j=3$	$j=4$	$j=5$
$i=200$	0.0072%	0.0273%	–0.1213%	–0.1260%	0.5706%
$i=100$	0.0233%	0.0274%	–0.1294%	–0.1324%	0.9202%
$i=75$	0.0406%	0.0298%	–0.1470%	–0.1454%	1.4118%
$i=50$	0.0924%	0.0505%	–0.2458%	–0.2152%	1.8360%
$i=25$	0.4228%	0.5165%	–1.8860%	–1.2860%	5.3230%

To further demonstrate the accuracy and advantages of the proposed discrete method, the Monte Carlo simulation method is introduced for the purpose of comparison. Here, Monte Carlo(x) represents a Monte Carlo simulation setting the number of trials to x. PLF(x) represents a discrete PLF method setting the number of sampling points to x.

The cumulative distribution curves (CDCs) of V_1 in the previous case under the first Pareto solution in Table 2 obtained by different methods are shown in Figure 7. As can be seen, the CDC of PLF(200) is much closer to Monte Carlo(5000) than the CDC of PLF(50).

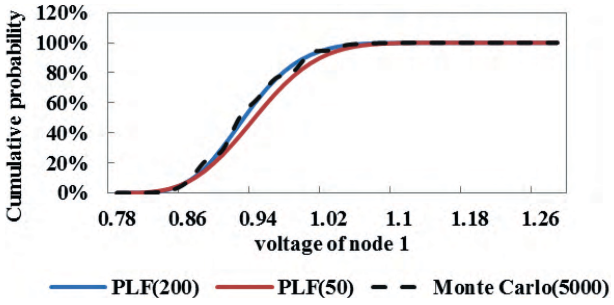

Figure 7. CDC of V1 obtained by different methods.

In each simulation of the Monte Carlo method, a set of deterministic values is assigned to random variables generated in accordance with the PDs of state vector. In this way, with the increasing number of trials, the Monte Carlo method gives a more precise result. In this paper, the simulation result of Monte Carlo(5000) is considered as the real PD of the V_1. ARMS is adopted [11]:

$$ARMS = \frac{\sqrt{\sum_{i=1}^{N}\left(f_{PLF}^{i} - f_{MC}^{i}\left(5000\right)\right)^{2}}}{N}, \tag{42}$$

where f_{PLF}^{i} and f_{MC}^{i} are the cumulative probability of V_1 at point i calculated with PLF and Monte Carlo(5000), respectively. The voltage points are located uniformly from 0.5 pu to 1.8 pu, and the number of voltage points is N = 130.

In this paper, the objective function algorithm is used to calculate virtual fitness of chromosomes in the procedure of NSGA-II. To ensure practicality, the objective function algorithm must be able to execute fast probability calculations, while ensuring a relatively high accuracy.

As can be seen from Table 5, with the increasing of the number of sampling points, the accuracy and execution time of PLF increase significantly. If the number of sampling points is 200, the corresponding ARMS is less than 0.01, and the execution time is only the equivalent of 12% of the simulation time of Monte Carlo(5000). Obviously, PLF(200) used in the previous NSGA-II optimization process is very appropriate.

Table 5. Simulation time and ARMS of the discrete PLF proposed in this paper.

Method	PLF(20)	PLF(50)	PLF(100)	PLF(200)	Monte Carlo(5000)
time/s	79	97	120	147	1230
ARMS	0.485	0.0792	0.0152	0.0081	0

7. Conclusions and outlook

In this paper, a quantitative configuration model of a hybrid wind and solar system is proposed. The premise of the model is that all random variables of the system must be independent of each other, but in terms of the actual system, this is sometimes too idealistic. In future research, the quantitative capacity configuration of a hybrid system involving correlated random variables will be discussed.

The simulation platform in this paper is a PC equipped with a pair of Intel Xeon 2.33 GHz quad-core CPU and 8 GB DDR3 memory. The speedup factor [20] of the NSGA-II with the population size of 50 and maximum evolution generation of 50 run parallelly on 8 processors reached 12.32. To further enhance optimization speed, we plan to use computer clusters to replace the current single machine with multicore mode.

References

[1] Arriaga M, Canizares CA, Kazerani M. Renewable energy alternatives for remote communities in Northern Ontario, Canada. IEEE T Sustain Energ 2013; 4: 661–670.

[2] Katti PK, Khedkar MK. Alternative energy facilities based on site matching and generation unit sizing for remote area power supply. Renew Energ 2007; 32: 1346–1362.

[3] Atwa YM, El-Saadany EF, Salama MMA, Seethapathy R. Optimal renewable resources mix for distribution system energy loss minimization. IEEE T Power Syst 2010; 25: 360–370.

[4] Chen Z, Spooner E. Grid power quality with variable speed wind turbines. IEEE T Energy Conver 2001; 16: 148–154.

[5] Kamyab E, Javad Sadeh. Islanding detection method for photovoltaic distributed generation based on voltage drifting. IET Generation, Transmission & Distribution 2013; 7: 584–592.

[6] Yousefian R, Monsef H. DG-allocation based on reliability indices by means of Monte Carlo simulation and AHP. In: IEEE 2003 Power Tech Conference; 2003; Bologna, Italy. New York, NY, USA: IEEE. pp. 2029–2034.

[7] Borkowska B. Probabilistic load flow. IEEE T Power Ap Syst 1974; 93: 752–759.

[8] Allan RN, Al-Shakarchi MRG. Probabilistic a.c. load flow. P IEE 1976; 123: 531–536.

[9] Allan RN, Borkowska B, Grigg CH. Probabilistic analysis of power flows. P IEE 1974; 121: 1551–1556.

[10] Allan RN, Grigg CH, Al-Shakarchi MRG. Numerical techniques in probabilistic load flow problems. Int J Numer Meth Eng 1976; 10: 853–860.

[11] Pei Z, Lee ST. Probabilistic load flow computation using the method of combined cumulants and Gram-Charlier expansion. IEEE T Power Syst 2004; 19: 676–682.

[12] Tian WD, Sutanto D, Lee YB, Outhred HR. Cumulant based probabilistic power system simulation using Laguerre polynomials. IEEE T Energy Conver 1989; 4: 567–574.

[13] Habib MA, Said SAM, El-Hadidy MA, Al-Zaharna I. Optimization procedure of hybrid photovoltaic wind energy system. Energy 1999; 24: 919–929.

[14] Borowy BS, Salameh ZM. Methodology for optimally sizing the combination of a battery bank and PV array in a wind/PV hybrid system. IEEE T Energy Conver 1996; 11: 367–375.

[15] Ai B, Yang H, Shen H, Liao X. Computer-aided design of PV/wind hybrid system. Renew Energ 2003; 28: 1491–1512.

[16] Karaki SH, Chedid RB, Ramadan R. Probabilistic performance assessment of autonomous solar-wind energy conversion systems. IEEE T Energy Conver 1999; 14: 766–772.

[17] Wang CS, Zheng HF, Xie YH. Probabilistic power flow containing distributed generation in distribution system. Automation of Electric Power Systems 2005; 9: 39–44.

[18] Monahan JF. Numerical Methods of Statistics. 2nd revised edition. Cambridge, UK: Cambridge University Press, 2011.

[19] Deb K, Agrawal S, Pratap A, Agarwal S. A fast and elitist multi-objective genetic algorithm: NSGA-II. IEEE T Evolut Comput 2002; 6: 182–197.

[20] Li Y, Cao YJ, Liu ZY, Jiang QY. Dynamic optimal reactive power dispatch based on parallel particle swarm optimization algorithm. Computers and Mathematics with Applications 2009; 5: 1835–1842.

[21] Dhople S, Garcia A. Estimation of photovoltaic system reliability and performance metrics. IEEE T Power Syst 2012; 27: 554–563.

[22] Ribrant J, Bertling LM. Survey of failures in wind power systems with focus on Swedish wind power plants during 1997–2005. IEEE T Energy Convers 2007; 22: 167–173.